American Mineralogist, Volume 94, pages 190–199, 2009

New insights into the crystal structure and crystal chemistry of the zeolite phillipsite

G. Diego Gatta,[1,2,*] Piergiulio Cappelletti,[3] Nicola Rotiroti,[1,2] Carla Slebodnick,[4] and Romano Rinaldi[5]

[1]Dipartimento di Scienze della Terra, Università degli Studi di Milano, Via Botticelli 23, I-20133 Milano, Italy
[2]CNR-Istituto per la Dinamica dei Processi Ambientali, Milano, Italy
[3]Dipartimento di Scienze della Terra, Università Federico II, Via Mezzocannone 8, I-80134 Napoli, Italy
[4]Crystallography Laboratory, Department of Chemistry, Virginia Polytechnic Institute, Blacksburg, Virginia 24061, U.S.A.
[5]Dipartimento di Scienze della Terra, Università degli Studi di Perugia, Piazza Università 1, I-06100 Perugia, Italy

Abstract

The crystal-structure, crystal-chemistry, and low-temperature behavior of a natural phillipsite-Na from the "Newer Volcanic Suite," Richmond, Melbourne district, Victoria, Australia [$K_{0.75}(Na_{0.88}Ca_{0.57})_{\Sigma 1.45}(Al_{2.96}Ti_{0.01}Si_{5.07})_{\Sigma 8.04}O_{16}\cdot 6.2H_2O$ ($Z = 2$), $a = 9.9238(6)$, $b = 14.3145(5)$, $c = 8.7416(5)$ Å, $\beta = 124.920(9)°$, and $V = 1018.20(9)$ Å^3, space group $P2_1/m$], have been investigated by means of in situ single-crystal X-ray diffraction, thermogravimetric analysis, and electron microprobe analysis in the wavelength dispersive mode. Two accurate structural refinements have been obtained on the basis of single-crystal X-ray diffraction data collected at 298 and 100 K, with: $R_1(F)_{298K} = 0.035$, 3678 unique reflections with $F_o > 4\sigma(F_o)$ and 195 parameters, and $R_1(F)_{100K} = 0.035$, 3855 unique reflections, $F_o > 4\sigma(F_o)$ and 195 parameters. In both refinements, the residuals in the final difference Fourier maps are <1 e^-/Å^3. A configuration of the extra-framework population different from that reported in previous studies is found at room temperature, with two possible sites for potassium (K1 and K2), one sodium/calcium site (Ca), and seven independent sites partially occupied by water molecules (W1, W2, W3, W4, W4′, W5, and W6). The low-temperature refinement shows that the framework component of the phillipsite structure is maintained within the *T*-range investigated. However, a change in the configuration of the extra-framework content occurs at low temperature: the occupancy of site K2 drastically decreases, while that of site K1 increases, the Ca site is split into two sub-sites (Ca1 and Ca2) and the number of water molecule sites decreases to six (W1, W2, W3, W4, W5, and W6). The rearrangement of the extra-framework population at low temperature is likely due to the change in shape (and size) of the micropores by tetrahedral tilting. The evolution of the "free diameters" with temperature shows that an "inversion" of the ellipticity of the eight-membered ring channel along [010] occurs. The evolution of the unit-cell parameters with *T* (measured at 298, 250, 200, 150, and 100 K) shows a continuous and linear trend, without evident thermo-elastic anomalies. The axial and volume thermal expansion coefficients ($\alpha_j = l_j^{-1}\cdot\partial l_j/\partial T$, $\alpha_V = V^{-1}\cdot\partial V/\partial T$) between 100 and 298 K, calculated by weighted linear regression, yield the following values: $\alpha_a = 1.8(1) \times 10^{-5}$, $\alpha_b = 1.2(1) \times 10^{-5}$, $\alpha_c = 1.1(1) \times 10^{-5}$, and $\alpha_V = 3.7(1) \times 10^{-5}K^{-1}$. The thermal expansion of phillipsite is significantly anisotropic ($\alpha_a:\alpha_b:\alpha_c$ = 1.64:1.09:1).

Keywords: Zeolite, phillipsite, crystal chemistry, low temperature, single-crystal X-ray diffraction

Introduction

Phillipsite, a common natural zeolite with the ideal composition $K_2(Na,Ca_{0.5})_3(Al_5Si_{11}O_{32})\cdot 12H_2O$ (Passaglia and Sheppard 2001), is typically found in amygdaloidal vugs of massive volcanic rocks (e.g., basalt, leucitites), in palagonitic basalts and tuffs as an alteration product of volcanic glass, or in diagenetically altered sediments in "closed hydrologic systems" (e.g., saline lakes and hot spring deposits) and "open hydrologic systems" (e.g., soils and land surface deposits, burial diagenetic environments, deep-sea sediments) (Galli and Loschi-Ghittoni 1972; Gottardi and Galli 1985; Langella et al. 2001; Passaglia and Sheppard 2001; Sheppard and Hay 2001). Phillipsite is isotypic with harmotome [$Ba_2(Na,Ca_{0.5})Al_5Si_{11}O_{32}\cdot 12H_2O$, Rinaldi et al. 1974; Passaglia and Sheppard 2001], forming a continuous series with no compositional gap (Černý et al. 1977; Coombs et al. 1997; Armbruster and Gunter 2001; Passaglia and Sheppard 2001). Crystals of natural phillipsite are often found in spherical radial aggregates and are ubiquitously twinned (Černý 1964; Rinaldi et al. 1974) (cruciform single and double penetration twins on {001}, {021}, and {110}). Intergrowths with several other zeolites (e.g., faujasite, offretite, gismondine, garronite, and gobbinsite) have been reported (Rinaldi et al. 1975; Passaglia and Sheppard 2001, and references therein). Natural phillipsite

* E-mail: diego.gatta@unimi.it

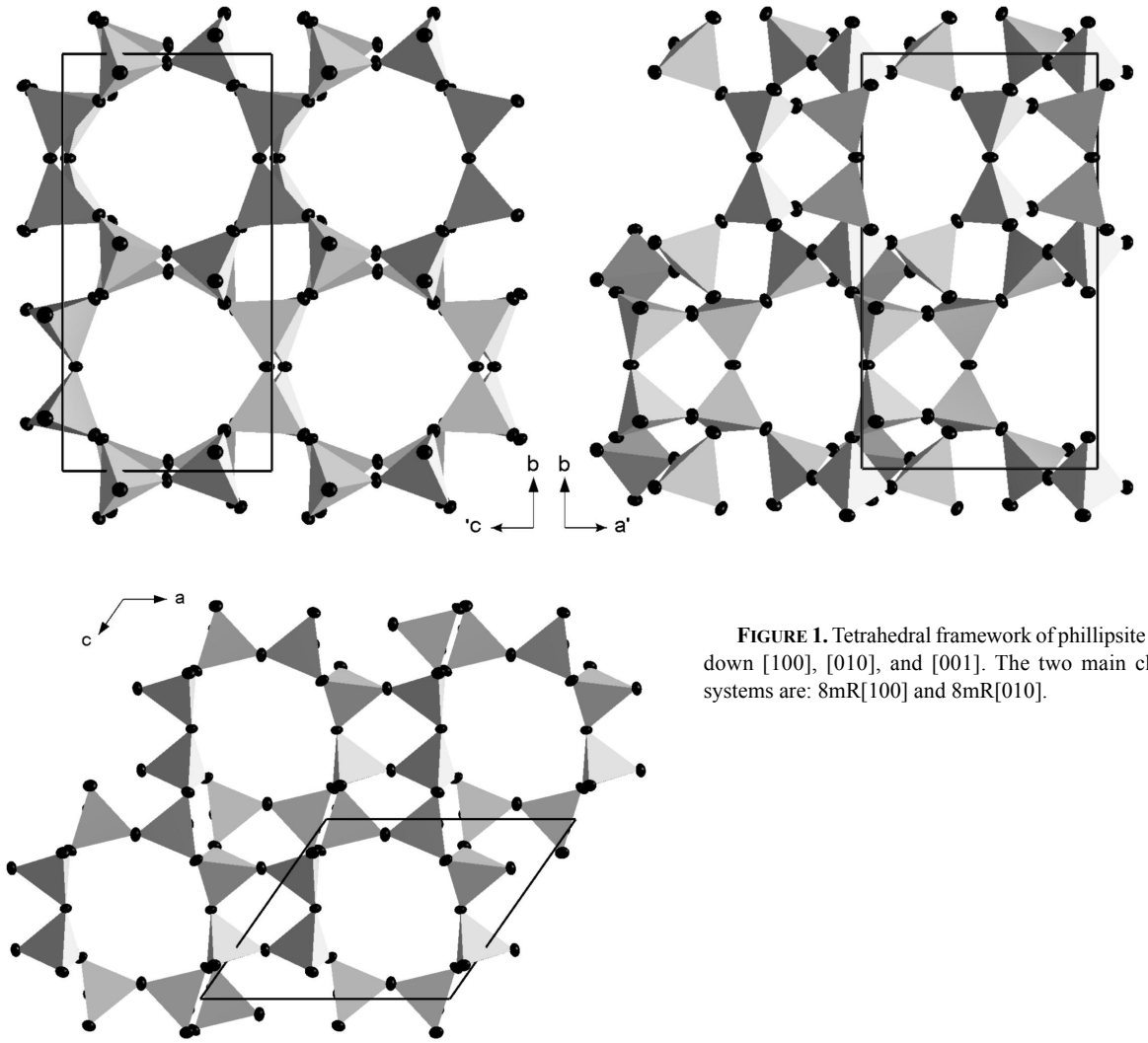

FIGURE 1. Tetrahedral framework of phillipsite viewed down [100], [010], and [001]. The two main channel-systems are: 8mR[100] and 8mR[010].

is monoclinic, space group $P2_1/m$, with $a \sim 9.865$, $b \sim 14.300$, $c \sim 8.693$ Å, $\beta \sim 124.81°$ (Rinaldi et al. 1974).

The Si/Al-tetrahedral framework of phillipsite is built up by four- and eight-membered rings, which represent the "secondary building units" (SBU code: 4 and 8; Framework Type: PHI, Baerlocher et al. 2001) (Fig. 1). The four-membered rings are connected to one-another throughout the framework in arrays of four double crankshaft chains (similar to those found in feldspars) running down the *a* axis. The eight-membered rings can also be thought of as sixfold connected double eight-membered rings (D8Rs), whereas normal D8Rs are eightfold connected. The PHI framework shows two main channel systems: an eight-membered ring channel along [100] (hereafter 8mR[100]) and an eight-membered ring channel along [010] (hereafter 8mR[010]) (Fig. 1). The two sets of channels intersect each other; the intersection can be thought of as a cage. The topological symmetry of the PHI framework type is orthorhombic, *Cmcm* ($a \sim 9.9$, $b \sim 14.1$, and $c \sim 14.0$ Å) with a low (ideal) framework density of 15.8 T/1000 Å^3 (Baerlocher et al. 2001). According to the structure refinement by Rinaldi et al. (1974), the Si/Al-distribution in the tetrahedral sites of phillipsite is random and the extra-framework population is represented by at least two cations sites, mainly occupied by K and Ca/Na, and five water-molecule sites. The K site was located in a peripheral position of the 8mR[100] (coordination number CN = 10, with K-$O_{max} \sim 3.4$ Å), whereas the Ca sites were located nearer the center of the channel (CN = 7, with Ca-$O_{max} \sim 3.0$ Å), above and below the mirror plane (Rinaldi et al. 1974). A more complex configuration of the extra-framework population in natural phillipsite was reported by Gualtieri et al. (1999a, 2000), on the basis of Rietveld refinements of synchrotron powder diffraction data.

The crystal chemistry of natural and NH_4^+-, Na^+-, K^+-, Cs^+-, Mg^{2+}-, Ca^{2+}-, Ba^{2+}-, and Sr^{2+}-exchanged specimens of phillipsite has been investigated, including some recent studies at high temperature and high pressure, by several authors (Steinfink 1962; Stuckenschmidt et al. 1990; Garcìa et al. 1992; Gualtieri 2000; Gualtieri et al. 1999a, 1999b, 2000; Passaglia et al. 2000; Sani et al. 2002; Gatta and Lee 2007). Due to its ion exchange selectivity for Cs^+ and Sr^{2+}, phillipsite is also considered a potential nuclear waste disposal material (Gualtieri et al. 1999a, 1999b). The thermal behavior of natural and cation-exchanged phillipsite, studied by thermogravimetric analysis, shows that the dehydra-

tion process is dependent on the nature of the extra-framework cations (Steinfink 1962; Passaglia et al. 2000). Two recent studies performed on the high-temperature structural evolution (Sani et al. 2002) and on the high-pressure elastic behavior and *P*-induced structural evolution (Gatta and Lee 2007) of phillipsite by in situ synchrotron X-ray powder diffraction, showed at least four high-temperature phases for phillipsite stable between 290 and 663 K (called phases "A," "B," "C," and "D") and a strongly anisotropic elastic behavior, without any evidence of phase transition, between 0.0001 and about 4 GPa.

The single-crystal and Rietveld powder diffraction refinements of natural phillipsite show significant differences in the extra-framework population compared to the structural model of Rinaldi et al. (1974), especially for sedimentary phillipsite. The model of Rinaldi et al. (1974) contains two symmetrically equivalent and mutually exclusive Ca sites and some unduly large thermal displacement parameters for some of the water O atoms. Unfortunately, the quality of the data at that time did not allow the authors to provide an unequivocal explanation for the large displacement ellipsoids that could only be ascribed to "the summation of the displacements of centers of motion (positions) plus the true thermal vibrations which tend to be large in zeolites" (Rinaldi et al. 1974, p. 2431). In actual fact, only the extra-framework sites were refined anisotropically to limit the number of refinement parameters.

The aim of this study is the reinvestigation of the crystal structure of a natural phillipsite also by means low-temperature data, to minimize the effects of thermal vibration and/or positional disorder and partial, alternative occupancy of the extra-framework sites.

The study was carried out by means of in situ single-crystal X-ray diffraction, thermogravimetric analysis (TG, DTG) and electron microprobe analysis in the wavelength dispersive mode (EPMA-WDS). Modern X-ray facilities and improvements in the other techniques (TG-DTG and EPMA-WDS) provide very accurate and precise data, allowing us to reinvestigate the crystal structure and crystal chemistry of open framework materials with complex extra-framework populations.

Sample description and mineralogy

A sample of natural phillipsite from the Newer Volcanic Suite, Richmond, Melbourne district, Victoria, Australia, was used for this study. Compared to phillipsite we analyzed from several different localities, phillipsite from Victoria gave the most suitable crystals for this study (i.e., absence of inclusions, twinning-free crystals, high-quality X-ray diffraction). Basalts from the Newer Volcanic Suite contain vesicles filled with different zeolite species (analcime, chabazite, gonnardite, natrolite, phillipsite, and thomsonite) (Vince 1989). Phillipsite and chabazite from the Burnley Quarries of the Newer Volcanic Suite were first reported in 1860. The basaltic rocks are dominated by tholeiitic compositions (Price et al. 1988) and contain iddingsitized olivine phenocrysts in a groundmass of plagioclase, clinopyroxene, olivine, and opaque oxides. Zeolites are invariably found in vesicles exhibiting a peculiar dome-like structure. Phillipsite is usually found in complex twinned crystals, with smaller crystals generally showing the simple forms such as fourling, prismatic and cruciform eightling, and clusters of these forms (Vince 1989). Varieties of the larger crystals include the "double-cross" first described by Ulrich (1870), clusters of this twinned form, and exceedingly complex rosettes, hemispheric radial aggregates and blocky aggregates. In fresh opened cavities, crystals of phillipsite are colorless and water-clear, but larger crystals soon become translucent to milky-white when allowed to dehydrate upon exposure (Vince 1989). Optical properties of the Richmond phillipsite have been studied by Langemann (1886) and Des Cloizeaux (1883). Phillipsite from Richmond quarries appear to be quite uniform in composition with Ca, Na, and K all varying within narrow limits and negligible Ba content. The mineral is classified as a phillipsite-Na (Coombs et al. 1997), because Na is the most abundant extra-framework cation. The coexisting chabazite is also a Na-rich variety (Birch 1989).

Experimental methods

Thermal analysis of the phillipsite sample was performed with a NETZSCH STA 449C instrument using 15.001 mg of powdered material ground in an agate mortar (grain size 10–15 μm). The temperature was raised up to 700 °C in air with increments of 1 °C/min. The total amount of H_2O, determined on the basis of the weight loss, is ~16.60 wt%.

Quantitative EPMA-WDS analyses were performed on polished single crystals, optically free of defects, using a Jeol JXA-8200 electron microprobe. The system was operated using a defocused electron beam (∅ 5 μm), an accelerating voltage of 15 kV, a beam current of 10 nA measured by a Faraday cup and counting times of 20 s on the peaks and 5 s on the backgrounds. Natural crystals of K-feldspar (for Si, K, Al), ilmenite (for Ti), forsterite (for Mg), fayalite (for Fe), wollastonite (for Ca), barite (for Ba), celestine (for Sr), and omphacite (for Na), were used as standards. The results were corrected for matrix effects using a conventional ZAF routine in the Jeol suite of programs. The crystals were found to be homogeneous within the analytical error. The chemical formula, obtained by averaging 10 point analyses, combined with the TG results and calculated on the basis of 16 O atoms, is the following:

$$K_{0.75}(Na_{0.88}Ca_{0.57})_{\Sigma=1.45}(Al_{2.96}Ti_{0.01}Si_{5.07})_{\Sigma=8.04}O_{16}\cdot 6.2H_2O\ (Z = 2).$$

Diffraction data were collected at 298 and 100 K using an Oxford Diffraction Gemini diffractometer, equipped with a Sapphire-III CCD detector and graphite monochromated Mo*K*α radiation (Enhance X-ray optics), operating at 50 kV and 40 mA. A combination of ω and φ scans was used to maximize the reciprocal space coverage (and redundancy), with a variable exposure time per frame (5 s/frame at 2θ ~ 0.2° and 50 s/frame at 2θ ~ 50°) and a crystal-detector distance of 50 mm (Table 1a). For the low-temperature data set, the crystal was slow-cooled to 100 K with a "Cryojet" open-flow nitrogen gas system (temperature stability better than 0.2 K and absolute uncertainty in temperature at the crystal position <2 K). Table 1a provides further details of the two data collections. The diffraction patterns at 298 and 100 K confirm a metrically monoclinic lattice with reflection conditions consistent with space group $P2_1/m$ (Rinaldi et al. 1974). No evidence of twinning was found. Lorentz-polarization and analytical absorption corrections, by Gaussian integration based upon the physical description of the crystal (CrysAlis, Oxford Diffraction 2007), were performed. The discrepancy factors between symmetry related diffraction intensities (Laue class 2/*m*) were R_{int} = 0.0473 at 298 K and R_{int} = 0.0437 at 100 K (Table 1a).

A second crystal of phillipsite, free of defects and without any evidence of twinning at the optical scale, was selected to describe the thermo-elastic behavior of this zeolite at low *T*. The crystal was cooled from 298 to 250 K (over ~8 min), from 250 to 200 K (over ~9 min), from 200 to 150 K (over ~14 min), and from 150 to 100 K (over ~37 min). Short data collections (~200 reflections) were performed at 298, 250, 200, 150, and 100 K, respectively, to measure the unit-cell constants at those temperatures, listed in Table 1b.

Results

Structure refinements at 298 and 100 K

The 298 K X-ray diffraction data of phillipsite were first processed with the program E-STATISTICS, implemented in

TABLE 1A. Details of data collection and refinement of phillipsite at 298 and 100 K

	298 K	100 K
Crystal size (μm³)	140 × 100 × 70	140 × 100 × 70
a (Å)	9.9238(6)	9.8511(12)
b (Å)	14.3145(5)	14.2476(14)
c (Å)	8.7416(5)	8.6422(10)
β (°)	124.920(9)	124.319(14)
V (Å³)	1018.20(9)	1001.81(19)
Space group	$P2_1/m$	$P2_1/m$
Radiation	Mo*K*α	Mo*K*α
Detector type	CCD	CCD
Crystal-detector distance (mm)	50	50
Scan type	ω/ϕ	ω/ϕ
Exposure time(s) at 2θ = 0.2°	5	5
Exposure time(s) at 2θ = 50.2°	50	50
2θ max (°)	80.05	80.51
	$-17 \le h \le 17$	$-16 \le h \le 17$
	$-25 \le k \le 24$	$-25 \le k \le 25$
	$-15 \le l \le 15$	$-15 \le l \le 15$
Coverage	>99.5%	>99.5%
Redundancy	3.5	3.5
No. measured reflections	23148	22933
No. unique reflections	6462	6418
No. unique reflections with $F_o > 4\sigma(F_o)$	3678	3855
No. refined parameters	195	195
R_{int}	0.0470	0.0437
R_1 *(F)* with $F_o > 4\sigma(F_o)$	0.0347	0.0351
wR_2 *(F²)*	0.0691	0.0675
GooF	1.020	1.060
Residuals (e^-/Å³)	+0.69/–0.45	+0.95/–0.67

Note: $R_{int} = \Sigma|F^2_{obs} - F^2_{obs}(mean)|/\Sigma[F^2_{obs}]$; $R_1 = \Sigma(||F_{obs}| - |F_{calc}||)/\Sigma|F_{obs}|$; $wR_2 = \{\Sigma[w(F^2_{obs} - F^2_{calc})^2]/\Sigma[w(F^2_{obs})^2]\}^{0.5}$, $w = 1/[\sigma^2(F^2_{obs}) + (a{\cdot}P)^2 + b{\cdot}P]$, $P = [\mathrm{Max}(F^2_{obs}, 0) + 2{\cdot}F^2_{calc}]/3$.

TABLE 1B. Unit-cell parameters of phillipsite at different temperatures

T (K)	*a* (Å)	*b* (Å)	*c* (Å)	β (°)	*V* (Å³)
298	9.909(8)	14.284(7)	8.715(7)	124.89(9)	1012(1)
250	9.898(8)	14.273(8)	8.709(7)	124.85(9)	1010(1)
200	9.890(7)	14.264(7)	8.707(6)	124.85(8)	1008(1)
150	9.880(7)	14.253(7)	8.702(7)	124.83(8)	1006(1)
100	9.874(6)	14.252(6)	8.695(6)	124.81(7)	1004.6(9)

the WinGX package (Farrugia 1999), to assign the real space group to phillipsite (i.e., $P2_1$ or $P2_1/m$). This program carries out a Wilson plot, calculates the normalized structure factors (E values) and the statistics of the distributions of these E values. The structure of phillipsite was found to be centrosymmetric at 82.6% likelihood. Furthermore, Sheldrick's $|E^2 - 1|$ criterion (Sheldrick 1997) also indicated that the structure is centrosymmetric ($|E^2 - 1| = 0.922$). The diffraction data were processed with the program ASSIGN-SPACEGROUP (in WinGX, Farrugia 1999), which compares the equivalent reflections under all possible Laue classes and provides a valuable check on the supposed Laue symmetry suggesting the actual space group. Two possible space groups (both belonging to Laue class 2/*m*) were selected by the program: $P2_1$ and $P2_1/m$. The combined figure of merit (CFOM) showed unambiguously that the space group $P2_1/m$ is more likely (CFOM-$P2_1/m$ = 1.971, CFOM-$P2_1$ = 8.734; the lower the value, the more likely the assignment).

The anisotropic structure refinement of the phillipsite data collected at 298 K was performed using the SHELX-97 software (Sheldrick 1997), starting from the atomic coordinates for the tetrahedral framework of Rinaldi et al. (1974) in space group $P2_1/m$. Neutral atomic scattering factors for Na, K, Ca, Si, and O were taken from the *International Tables for Crystallography* (Wilson and Prince 1999). A scattering curve based on partially occupied tetrahedral sites by Al and Si did not improve significantly the figures of merit of the refinement. Correction for secondary isotropic extinction was not necessary. The following strategy was used in the refinement. Atomic positions of the tetrahedral framework were refined first. Then, on the basis of the maxima in the difference-Fourier maps of the electron density, the extra-framework sites were assigned to K, Ca/Na, and O (water molecules), as reported in Table 2. The main differences with respect to the extra-framework configuration reported in Rinaldi et al. (1974) are the following: (1) the K site refined as

TABLE 2. Refined positional and thermal displacement parameters (Å²) of phillipsite at 298 K

Site (Wyck.)	*x*	*y*	*z*	Site occupancy	U_{11}	U_{22}	U_{33}	U_{23}	U_{13}	U_{12}	U_{eq}/U_{iso}
T1 (4*f*)	0.72527(4)	0.00683(2)	0.28477(4)	1.0	0.0123(1)	0.0156(1)	0.0122(1)	–0.0008(1)	0.0063(1)	0.0007(1)	0.01380(6)
T2 (4*f*)	0.42172(4)	0.13923(2)	0.04494(5)	1.0	0.0122(1)	0.0122(1)	0.0145(1)	–0.0003(1)	0.0067(1)	0.0010(1)	0.01350(6)
T3 (4*f*)	0.04307(4)	0.02522(2)	0.28043(5)	1.0	0.0142(1)	0.0139(1)	0.0112(1)	–0.0009(1)	0.0077(1)	–0.0017(1)	0.01287(6)
T4 (4*f*)	0.08288(4)	0.14052(2)	0.00296(5)	1.0	0.0166(1)	0.0112(1)	0.0156(1)	–0.0005(1)	0.0108(1)	–0.0009(1)	0.01359(6)
O1 (4*f*)	0.0615(1)	0.11290(7)	0.1724(1)	1.0	0.0347(5)	0.0237(4)	0.0235(5)	0.0036(4)	0.0207(4)	–0.0004(4)	0.0250(2)
O2 (4*f*)	0.6291(1)	0.58688(7)	0.1499(1)	1.0	0.0326(5)	0.0239(5)	0.0221(5)	0.0056(4)	0.0158(4)	0.0050(4)	0.0261(2)
O3 (4*f*)	0.5947(1)	0.09597(7)	0.2286(1)	1.0	0.0204(4)	0.0280(5)	0.0241(5)	–0.0010(4)	0.0067(4)	0.0072(3)	0.0276(2)
O4 (4*f*)	0.0399(1)	0.92452(7)	0.1868(1)	1.0	0.0306(6)	0.0196(4)	0.0251(5)	–0.0060(4)	0.0130(4)	–0.0006(3)	0.0267(2)
O5 (4*f*)	0.8771(1)	0.04490(7)	0.2722(1)	1.0	0.0247(4)	0.0282(5)	0.0331(5)	–0.0008(4)	0.0207(4)	–0.0015(4)	0.0262(2)
O6 (4*f*)	0.2793(1)	0.37402(8)	0.0853(2)	1.0	0.0237(5)	0.0350(6)	0.0358(6)	–0.0015(4)	0.0197(4)	–0.0020(4)	0.0299(2)
O7 (4*f*)	0.7927(1)	0.52202(7)	0.5036(1)	1.0	0.0211(4)	0.0333(5)	0.0152(4)	–0.0020(4)	0.0074(3)	0.0012(4)	0.0249(2)
O8 (2*e*)	0.5455(2)	3/4	–0.0257(2)	1.0	0.0360(7)	0.0148(6)	0.0336(8)	0	0.0211(7)	0	0.0275(3)
O9 (2*e*)	0.0224(2)	1/4	–0.0610(2)	1.0	0.0343(7)	0.0160(6)	0.0269(7)	0	0.0143(6)	0	0.0276(3)
K1 (2*e*)	0.8674(8)	1/4	0.226(1)	0.58(4)	0.078(2)	0.023(1)	0.065(2)	0	0.042(1)	0	0.0543(8)
K2 (2*e*)	0.8451(6)	1/4	0.187(5)	0.30(4)	0.057(4)	0.035(2)	0.112(7)	0	0.064(5)	0	0.059(3)
Ca (4*f*)	0.6682(1)	0.37452(8)	0.5593(1)	0.521(3)	0.0334(5)	0.0416(6)	0.0267(5)	–0.0075(4)	0.0199(4)	–0.0131(4)	0.0324(3)
W1 (2*e*)	1.2177(4)	1/4	0.5627(4)	0.91(1)	0.130(3)	0.042(2)	0.047(2)	0	0.036(2)	0	0.081(1)
W2 (2*e*)	0.2129(3)	3/4	0.4774(4)	0.95(1)	0.060(2)	0.127(3)	0.039(2)	0	0.007(1)	0	0.088(2)
W3 (4*f*)	0.3513(3)	0.6450(3)	0.1717(4)	0.87(1)	0.070(2)	0.180(4)	0.095(2)	–0.006(2)	0.055(2)	0.005(2)	0.110(2)
W4 (4*f*)	0.582(3)	0.786(4)	0.568(1)	0.29(6)	0.032(6)	0.093(14)	0.047(4)	–0.008(3)	0.008(3)	0.003(6)	0.066(6)
W4′ (4*f*)	0.545(9)	0.735(2)	0.551(8)	0.14(6)							0.051(8)
W5 (4*f*)	0.5209(8)	0.9854(5)	0.5421(9)	0.432(7)	0.076(4)	0.116(6)	0.096(6)	0.042(4)	0.071(4)	0.009(3)	0.084(2)
W6 (4*f*)	0.5984(9)	0.8864(9)	0.5662(9)	0.30(1)	0.075(5)	0.189(12)	0.058(5)	0.064(5)	–0.008(3)	–0.070(6)	0.133(7)

Notes: The anisotropic displacement factor exponent takes the form: $-2\pi^2[(ha^*)^2U_{11} + \cdots + 2hka^*b^*U_{12}]$. U_{eq} is defined as one third of the trace of the orthogonalized U_{ij} tensor. For the T1, T2, T3, and T4 sites the scattering curve of silicon (neutral) was used. For the K1 and K2 sites the scattering curve of potassium was used, whereas for the Ca site a mixed scattering curve (30%Ca + 70%Na) was adopted. W4′ was refined isotropically because of the low site occupancy.

two partially occupied, mutually exclusive sites, ~0.28 Å apart, here labeled K1 and K2 (Figs. 2 and 3, Table 2). A similar finding was actually reported for the isotropic refinement by Rinaldi et al. (1974); and (2) seven independent sites are assigned to water molecules (here labeled as W1, W2, W3, W4, W4′, W5, and W6); only two of them (W1 and W2) lie at the Wyckoff special positions 2*e*, the W4 site is split into two sub-sites ~0.43 Å apart with partial occupancies (W4 and W4′), (Fig. 2, Table 2).

The sites were labeled to maintain, as much as possible, the labeling scheme used by Rinaldi et al. (1974). A mixed scattering curve was used for the Ca site. The best fit was achieved with (30%Ca + 70%Na). Using the aforementioned structural model (Table 2), convergence was rapidly achieved after a few least-square cycles of refinement and the variance-covariance matrix did not show any significant correlation among the refined parameters. At the end of refinement, the residual electron density in the difference-Fourier maps was between +0.69 and –0.45 e^-/Å^3 with an agreement factor $R_1(F)$ = 0.0347 based on 3678 unique reflections with $F_o > 4\sigma(F_o)$ and 195 refined parameters (Table 1a).

The space group assignment and structure refinement for the 100 K structure were carried out using the same protocol as used for the 298 K structure. The figures of merit from the programs E-STATISTICS and ASSIGN-SPACEGROUP (in WinGX, Farrugia 1999) showed that the space group $P2_1/m$ is maintained. After the refinement of the framework sites, a careful inspection of the difference-Fourier maps shows a slightly different configuration of the extra-framework population than that found at 298 K. In particular: (1) the Ca site refined as two sub-sites with partial, mutually exclusive occupancy (Fig. 4), here labeled Ca1 (close to the position of the Ca site at 298 K) and Ca2, ~1.12 Å distant (Fig. 2, Table 3); and (2) the W4′ site was empty (Fig. 2, Table 3).

When convergence was reached, the residual electron density in the difference-Fourier maps was between +0.95 and –0.67 e^-/Å^3 with an agreement factor $R_1(F)$ = 0.0351 based on 3855 unique reflections with $F_o > 4\sigma(F_o)$ and 195 refined parameters (Table 1a).

Low-*T* elastic behavior

The variation of the unit-cell parameters of phillipsite as a function of *T* are shown in Figure 5. Each trend is continuous and linear, showing no thermo-elastic anomaly within the *T*-range investigated. The axial and volume thermal expansion coefficients

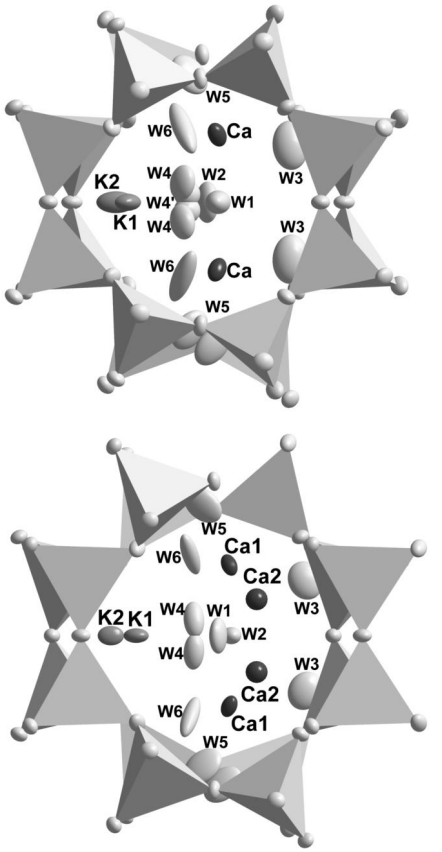

FIGURE 2. Configuration of the extra-framework population in phillipsite, as viewed down [100], based on the structural refinements at 298 K (above) and at 100 K (below). Thermal ellipsoid probability factor: 50%.

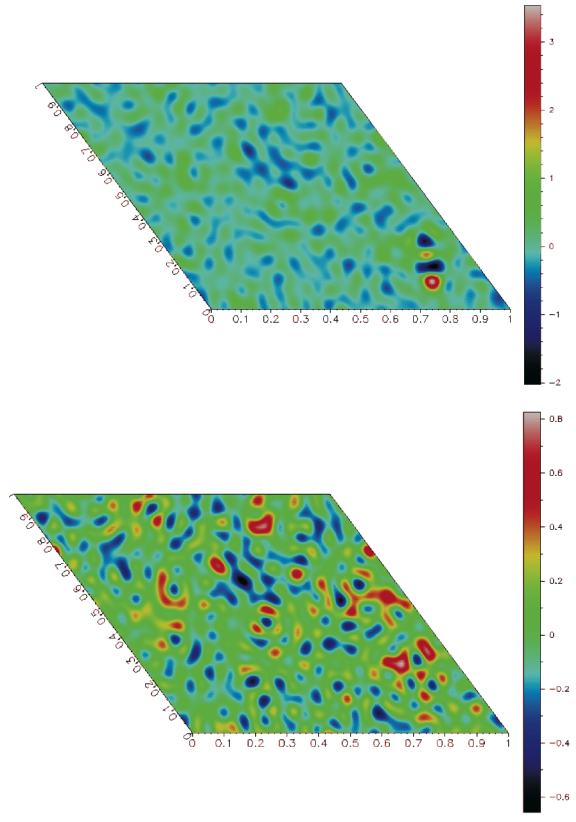

FIGURE 3. Difference Fourier maps of the electron density (e^-/Å^3) of phillipsite at y = 1/4 (above) after the first cycles of refinement at 298 K without the K2 site, showing one intense positive residual peak at x ~ 0.84, z ~ 0.14, and (below) after the assignment of the K2 site. (Note: the color scale is different for the two maps; map orientation: x positive to the right.)

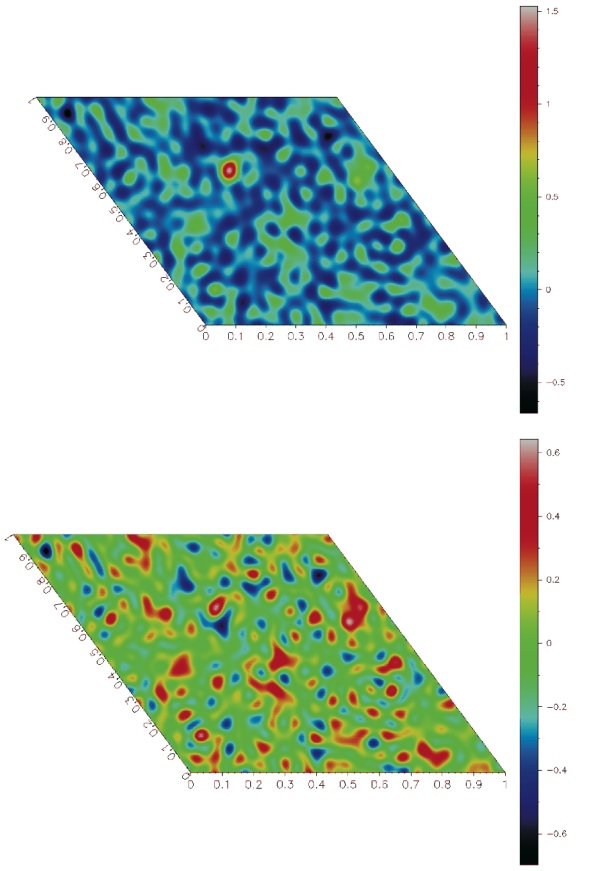

FIGURE 4. Difference Fourier maps of the electron density (e^-/Å^3) of phillipsite at $y \sim 0.31$ (above) after the first cycles of refinement at 100 K without the Ca2 site, showing one intense positive residual peak at $x \sim 0.46$, $z \sim 0.66$, and (below) after the assignment of the Ca2 site. (Note: the color scale is different for the two maps; map orientation: x positive to the right.)

($\alpha_j = l_j^{-1} \cdot \partial l_j / \partial T$, $\alpha_V = V^{-1} \cdot \partial V / \partial T$) between 100 and 298 K were calculated by weighted linear regression, yielding the following values: $\alpha_a = 1.8(1) \times 10^{-5}$, $\alpha_b = 1.2(1) \times 10^{-5}$, $\alpha_c = 1.1(1) \times 10^{-5}$, $\alpha_V = 3.7(1) \times 10^{-5}$K^{-1}. The thermal expansion of phillipsite is significantly anisotropic, with α_a:α_b:α_c = 1.64:1.09:1.

The monoclinic symmetry of phillipsite (here described in the *b*-unique setting) makes the axial thermal expansion along the *b*-axis the only one parallel to one of the three axes of the thermo-elastic unit-strain ellipsoid. Magnitude and orientation of the Lagrangian unit-strain ellipsoid between 298 and 100 K were then calculated with the software STRAIN (Ohashi 1982), using the calculated unit-cell parameters at 298 and 100 K on the basis of the linear regression through the data points (Fig. 5). The values of the principal unit-strain coefficients (ε1, ε2, ε3, with |ε1| < |ε2| < |ε3|) are: $\varepsilon 1 = 0.7(2) \times 10^{-5}$, $\varepsilon 2 = 1.2(2) \times 10^{-5}$, $\varepsilon 3 = 1.8(1) \times 10^{-5}$K^{-1}. The unit-strain ellipsoid is oriented with the ε2 axis parallel to [010], ε1 and ε3 lying in the (010) plane with ε1∠[100] = 85(8)° and ε1∠[001] = 39(8)°. The ori-

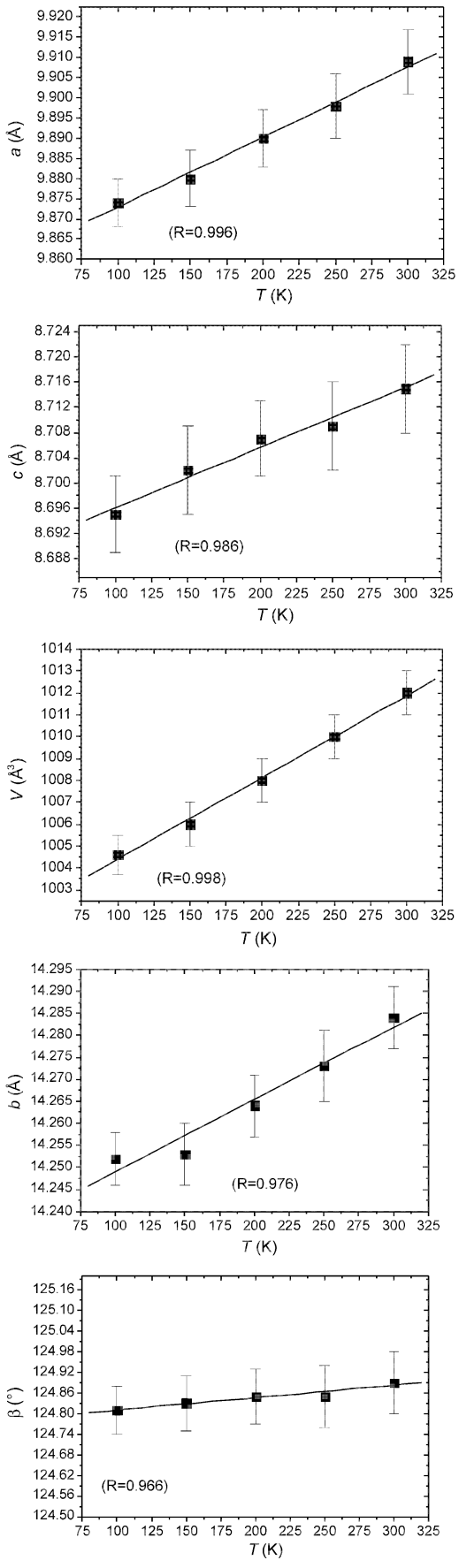

► **FIGURE 5.** Evolution of the unit-cell parameters of phillipsite with *T*. The solid lines represent the weighted regression curves through the data points.

TABLE 3. Refined positional and thermal displacement parameters (Å^2) of phillipsite at 100 K

Site (Wyck.)	*x*	*y*	*z*	Site occupancy	U_{11}	U_{22}	U_{33}
T1 (4*f*)	0.73740(4)	0.02709(2)	0.28032(4)	1.0	0.00852(12)	0.00999(12)	0.00851(12)
T2 (4*f*)	0.42066(4)	0.14079(2)	–0.00085(5)	1.0	0.01106(12)	0.01159(13)	0.00986(12)
T3 (4*f*)	0.06192(4)	0.00519(2)	0.28590(4)	1.0	0.01106(12)	0.01159(13)	0.00986(12)
T4 (4*f*)	0.12529(4)	0.13921(2)	0.04726(4)	1.0	0.01173(13)	0.00958(12)	0.01115(13)
O1 (4*f*)	0.13911(13)	0.09415(7)	0.23177(14)	1.0	0.0293(5)	0.0225(5)	0.0188(4)
O2 (4*f*)	0.64477(12)	0.57363(7)	0.18824(14)	1.0	0.0232(4)	0.0147(4)	0.0203(4)
O3 (4*f*)	0.61319(10)	0.11578(7)	0.16950(13)	1.0	0.0138(4)	0.0167(4)	0.0179(4)
O4 (4*f*)	0.02204(11)	0.91187(7)	0.14892(13)	1.0	0.0198(4)	0.0193(4)	0.0166(4)
O5 (4*f*)	0.89803(11)	0.04451(7)	0.27452(14)	1.0	0.0160(4)	0.0207(5)	0.0232(4)
O6 (4*f*)	0.30724(12)	0.37356(8)	0.08322(15)	1.0	0.0196(4)	0.0280(5)	0.0293(5)
O7 (4*f*)	0.78704(11)	0.47439(7)	0.49591(12)	1.0	0.0189(4)	0.0253(5)	0.0121(4)
O8 (2*e*)	0.58790(18)	3/4	0.0709(2)	1.0	0.0282(7)	0.0152(6)	0.0186(6)
O9 (2*e*)	0.07278(17)	1/4	0.0317(2)	1.0	0.0222(6)	0.0127(6)	0.0251(7)
K1 (2*e*)	0.85967(16)	1/4	0.2279(4)	0.796(8)	0.0300(4)	0.0147(3)	0.0432(10)
K2 (2*e*)	0.822(2)	1/4	0.138(4)	0.075(8)	0.023(5)	0.026(3)	0.047(11)
Ca1 (4*f*)	0.39299(10)	0.37620(7)	0.5585(12)	0.507(3)	0.0152(4)	0.0318(5)	0.0192(4)
Ca2 (4*f*)	0.4560(19)	0.3150(11)	0.656(2)	0.065(5)			
W1 (2*e*)	1.2322(3)	1/4	0.5194(3)	0.895(10)	0.0521(15)	0.089(2)	0.0222(11)
W2 (2*e*)	0.1594(2)	3/4	0.4340(3)	0.873(8)	0.0419(12)	0.0204(9)	0.0276(11)
W3 (4*f*)	0.3190(3)	0.8485(2)	0.1715(4)	0.748(8)	0.0485(14)	0.101(2)	0.083(2)
W4 (4*f*)	0.4937(4)	0.7787(3)	0.5669(4)	0.393(6)	0.0303(17)	0.088(5)	0.0295(17)
W5 (4*f*)	0.5196(6)	0.9840(5)	0.5356(10)	0.441(7)	0.031(3)	0.092(5)	0.100(5)
W6 (4*f*)	0.4852(8)	0.8954(6)	0.5800(7)	0.277(8)	0.084(5)	0.111(7)	0.029(3)

Notes: The anisotropic displacement factor exponent takes the form: $-2\pi^2[(ha^*)^2U_{11}+\ldots+2hka^*b^*U_{12}]$. U_{eq} is defined as one third of the trace of the orthogonalized U_{ij} tensor. For the T1, T2, T3, and T4 sites the scattering curve of silicon (neutral) was used. For the K1 and K2 sites the scattering curve of potassium was used, whereas for the Ca1 and Ca2 sites a mixed scattering curve (30%Ca + 70%Na) was adopted. Ca2 was refined isotropically because of the low site occupancy.

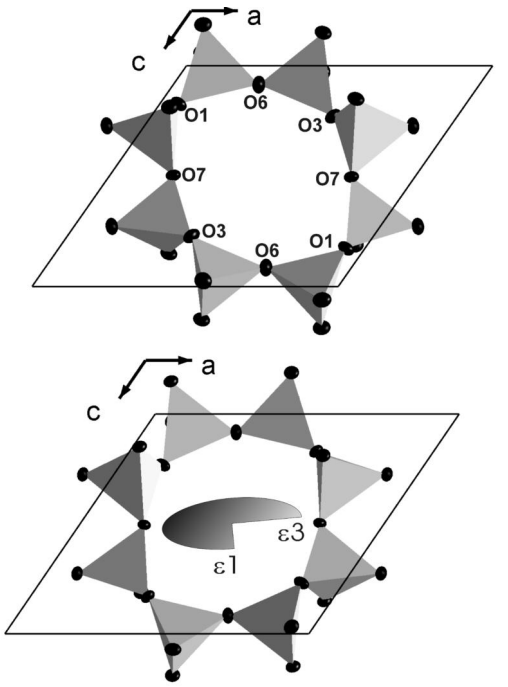

FIGURE 6. Configuration of the 8mR[010] at 298 K (above) and 100 K (below). The orientation of the Lagrangian unit-strain ellipsoid, calculated between 298 and 100 K, is shown (ε_2 // [010], $|\varepsilon_3| > |\varepsilon_2| > |\varepsilon_1|$).

entation of the unit-strain ellipsoid is schematically shown in Figure 6. The thermo-elastic anisotropy between 298 and 100 K is significantly higher than that along the principal unit-cell edges, with $\varepsilon1:\varepsilon2:\varepsilon3 = 1:1.71:2.57$.

DISCUSSION AND CONCLUDING REMARKS

As reported in several studies (Passaglia and Sheppard 2001, and references therein), phillipsite shows a very wide range of Si/(Si + Al), K/(K + Ba), and Na/(Na + Ca) ratios, reflecting a relationship between chemical composition and different genetic environments (Alberti 1978). Variations in the extra-framework population results from factors such as post-formational exchange processes (de'Gennaro et al. 1982), peculiar chemical composition of the precursor reacting glass, or chemical composition of the fluids interacting with this precursor (de'Gennaro et al. 1999). In the light of these considerations, accurate structure refinements of chemically different specimens of phillipsite are highly desirable. In this study, the direct comparison of the 298 and 100 K structures of Na-rich phillipsite from Richmond provides new insight into the crystal structure and low-*T* behavior of this zeolite, particularly with respect to the complex configuration of the extra-framework population.

Comparison between the 298 K and the 100 K phillipsite structures shows that the tetrahedral framework is maintained within the *T*-range investigated; slight differences among the intra-tetrahedral bond distances and angles can be ascribed to the effect of temperature (Tables 4, 5, and 6) and/or to the change in the configuration of the extra-framework content, with a consequent change in framework/extra-framework bonding. At room temperature, the extra-framework population consists of two partially occupied, mutually exclusive, potassium sites (K1 and K2), one partially occupied calcium/sodium site (Ca), and seven water sites (W1, W2, W3, W4, W4′, W5, W6). The coordination-shells of potassium (K1 and K2 sites) are large and distorted polyhedra with coordination number CN = 9 (five framework O atoms + four H_2O molecules) (Table 4). The coordination shell of the Ca site is more complex, with at least nine possible mutually exclusive configurations, with CN = 6 – 7 (three framework O atoms + four H_2O molecules, labeled as "a," "b," "c," "d," "e," "f," "g," and "h," and three framework O atoms + three H_2O molecules, labeled as "i" in Table 4).

In comparison to the room-temperature structure, the arrangement of the extra-framework population at 100 K shows CN =

TABLE 3.—*EXTENDED*

U_{23}	U_{13}	U_{12}	U_{eq}/U_{iso}
–0.00092(11)	0.00352(10)	0.00073(10)	0.00971(6)
–0.00032(11)	0.00619(10)	–0.00117(10)	0.01058(6)
–0.00032(11)	0.00619(10)	–0.00117(10)	0.01068(6)
0.00008(11)	0.00739(11)	–0.00097(10)	0.01030(6)
–0.0012(4)	0.0157(4)	–0.0077(4)	0.02237(19)
0.0037(3)	0.0108(4)	0.0033(3)	0.02025(18)
0.0020(3)	0.0045(3)	0.0026(3)	0.01856(17)
–0.0028(3)	0.0070(4)	–0.0004(3)	0.02034(18)
–0.0010(4)	0.0115(4)	0.0011(3)	0.01971(18)
–0.0007(4)	0.0169(4)	0.0001(4)	0.0239(2)
–0.0016(3)	0.0079(3)	–0.0031(3)	0.01927(17)
0	0.0110(5)	0	0.0219(3)
0	0.0110(5)	0	0.0212(3)
0	0.0196(5)	0	0.0299(4)
0	0.027(7)	0	0.028(4)
–0.0068(3)	0.0071(3)	0.0023(3)	0.0235(3)
			0.058(6)
0	0.0222(11)	0	0.0537(10)
0	0.0110(8)	0	0.0347(7)
0.0116(15)	0.0476(14)	0.0033(12)	0.0717(12)
0.0040(16)	0.0154(13)	–0.0094(15)	0.0499(18)
0.035(3)	0.037(3)	0.0298(19)	0.074(2)
0.031(3)	0.035(3)	0.076(4)	0.073(3)

9 for the K1 site and CN = 8 for the K2 site (five framework O atoms + four H_2O molecules for K1; six framework O atoms + two H_2O molecules for K2). At least three possible and statistically distributed configurations (labeled "a," "b," and "c" in Table 5) may be inferred for each of the two Ca sites identified in the refinement. The Ca1 polyhedron, with CN = 7, has three framework O atoms and four H_2O molecules. The Ca2 polyhedron, also with CN = 7, has two framework O atoms and five H_2O molecules (Table 5). One of the most significant changes in the extra-framework population at low *T*, compared to room temperature, is represented by the different K1 and K2 site occupancies (S) (Tables 2 and 3): S(K1) ~58% and S(K2) ~30% at 298 K and S(K1) ~80% and S(K2) ~8% at 100 K. In other words, the K2-site tends to disappear with decreasing temperature. Two K sites, ~0.4 Å apart, were in fact postulated in the isotropic refinement at room temperature by Rinaldi et al. (1974). The present refinements precisely locate these sites.

The unit-formula based on the structure refinement at room temperature, using the scattering curve of potassium at the K1 and K2 sites and a mixed curve (30%Ca + 70%Na) at the Ca site, becomes $^{K1,K2}K^{Ca}_{0.88}(Na,Ca)_{\Sigma 1.05}T_8O_{16}\cdot 5.9H_2O$. At 100 K, the refinement yields $^{K1,K2}K^{Ca1,Ca2}_{0.87}(Na,Ca)_{\Sigma 1.15}T_8O_{16}\cdot 5.5H_2O$. The refined amount of water at both 298 and 100 K is slightly lower than that of the thermogravimetric analysis, i.e.,

$$K_{0.75}(Na_{0.88}Ca_{0.57})_{\Sigma=1.45}(Al_{2.96}Ti_{0.01}Si_{5.07})_{\Sigma=8.04}O_{16}\cdot 6.2H_2O.$$

Structure refinements and chemical data are in good agreement pointing to a potassium content ranging between 0.75 and 0.88 apfu. In other words, the K site is not fully occupied by potassium. A more significant difference between refinements and chemical analysis concerns the population of the Ca site (1.05 and 1.15 vs. 1.45 apfu, respectively). This could mean that a certain amount of calcium or sodium share the K1 and/or K2 site with potassium, even though the refined cation-oxygen bond-distances (i.e., K1-O_n and K2-O_n, Table 2) are not ideal for Ca^{2+} or Na^+. Based on the atomic distances and displacement parameters for the extra-framework sites (Table 2) it seems unlikely that any of the sites assigned to the water molecules are occupied by sodium or calcium, although this remains a possibility based solely on scattering power considerations. Therefore a multi-element distribution is likely to occur at the extra-framework cationic sites, leading to the following general chemical formula for phillipsite-Na:

$$^{K1,K2}(K,Na,Ca_{0.5})^{Ca}(Na,Ca_{0.5})_2{}^{T}(Al_3Si_5)O_{16}\cdot 6H_2O.$$

This could explain the lower amount of $Na^+ + Ca^{2+}$ refined in the Ca site as compared to the amount obtained by chemical analysis (i.e., 1.05–1.15 vs. 1.45 apfu) and the higher amount of K^+ refined in the K1 and K2 sites as compared to the amount obtained by chemical analysis (i.e., 0.87–0.88 vs. 0.75 apfu). In the previous single-crystal refinement of a natural phillipsite from Casal Brunori (Rome), Rinaldi et al. (1974) considered the K site fully occupied by potassium and found an amount of Na^+

TABLE 4. Relevant bond distances (Å) in the phillipsite structure at 298 K

						"a"	"b"	"c"	"d"	"e"	"f"	"g"	"h"	"i"
T1-O5	1.6641(10)	K1-O5(×2)	2.958(1)	Ca-W6	2.216(8)									i
T1-O2	1.6769(10)	K1-O1(×2)	2.968(3)	Ca1-W5(I)	2.218(7)	a	b	c	d					
T1-O7	1.6774(10)	K1-W1	3.006(8)	Ca-W2	2.260(2)	a	b	c	d	e	f	g	h	i
T1-O3	1.6795(10)	K1-W2	3.121(6)	Ca-W4′(I)	2.35(5)		b				f			
<T1-O>	1.6745	K1-W3(×2)	3.225(8)	Ca-W4 (I)	2.415(11)	a				e				
T2-O8	1.6464(5)	K1-O8	3.413(6)	Ca-W5 (II)	2.435(7)					e	f	g	h	
T2-O6	1.6516(10)			Ca-W3	2.484(3)	a	b	c	d	e	f	g	h	i
T2-O2	1.6535(10)			Ca-O4	2.543(1)	a	b	c	d	e	f	g	h	i
T2-O3	1.6589(10)			Ca-O3	2.579(1)	a	b	c	d	e	f	g	h	i
<T2-O>	1.6526	K2-O1(×2)	2.966(4)	Ca-O7	2.628(1)	a	b	c	d	e	f	g	h	i
T3-O5	1.6314(10)	K2-W3(×2)	2.98(3)	Ca-W4′(II)	2.65(6)			c				g		
T3-O7	1.6429(10)	K2-O5(×2)	3.001(7)	Ca-W4 (II)	3.08(6)				d				h	
T3-O1	1.6430(10)	K2-W1	3.25(3)											
T3-O4	1.6493(10)	K2-O8	3.28(1)											
<T3-O>	1.6416	K2-W2	3.30(2)											
T4-O9	1.6568(6)													
T4-O1	1.6592(10)													
T4-O6	1.6601(10)													
T4-O4	1.6701(10)													
<T4-O>	1.6615													

Note: Nine possible and mutually exclusive configurations for the Ca1 polyhedron (labeled as "a," "b," …, "i") are reported (see text for details).

TABLE 5. Relevant bond distances (Å) in the phillipsite structure at 100 K

						"a"	"b"	"c"
T1-O5	1.6301(9)	K1-O3(×2)	2.903(1)	Ca1-W5 (I)	2.132(7)		b	
T1-O2	1.6452(10)	K1-O5(×2)	2.950(1)	Ca1-W6	2.137(5)	a		
T1-O7	1.6382(9)	K1-W2	3.032(3)	Ca1-W1	2.2918(18)	a	b	c
T1-O3	1.6400(10)	K1-W1	3.064(3)	Ca1-W4 (I)	2.390(3)		b	
<T1-O>	1.6384	K1-W3(×2)	3.182(4)	Ca1-W5 (II)	2.418(6)			c
T2-O8	1.6545(6)	K1-O9	3.360(2)	Ca1-W3	2.487(3)	a	b	c
T2-O6	1.6532(10)			Ca1-O2	2.5215(13)	a	b	c
T2-O2	1.6663(10)			Ca1-O1	2.5384(15)	a	b	c
T2-O3	1.6562(10)			Ca1-O7	2.6377(14)	a	b	c
<T2-O>	1.6575	K2-W3(×2)	2.62(3)	Ca1-W4 (II)	2.942(4)	a		c
T3-O5	1.6586(9)	K2-O3(×2)	2.929(6)					
T3-O7	1.6729(10)	K2-O5(×2)	3.086(10)	Ca2-W3 (I)	1.907(16)	a	b	c
T3-O1	1.6747(10)	K2-O9	3.086(10)	Ca2-W1	2.044(16)	a	b	c
T3-O4	1.6730(10)	K2-O8	3.367(15)	Ca2-W4 (I)	2.303(16)		b	c
<T3-O>	1.6698			Ca2-W4 (II)	2.611(16)	a		
T4-O9	1.6428(5)			Ca2-O2	2.611(16)	a	b	c
T4-O1	1.6519(10)			Ca2-W6	2.673(16)	a		
T4-O6	1.6475(10)			Ca2-O8	2.786(16)	a	b	c
T4-O4	1.6541(10)			Ca2-W3 (II)	2.972(16)	a	b	c
<T4-O>	1.6491			Ca2-W5	3.007(18)		b	
				Ca2-W5 (I)	3.227(2)			c

Note: Three possible and mutually exclusive configurations for the Ca1 and Ca2 polyhedron (labeled as "a," "b," and "c", respectively) are reported (see text for details).

TABLE 6. Tetrahedral bond angles (°) in the phillipsite structure at 298 and 100 K

298 K		100 K	
O5-Si1-O2	112.84(5)	O5-Si1-O2	113.65(5)
O5-Si1-O7	111.77(5)	O5-Si1-O7	111.37(5)
O2-Si1-O7	107.45(5)	O2-Si1-O7	105.51(5)
O5-Si1-O3	107.96(5)	O5-Si1-O3	106.41(5)
O2-Si1-O3	111.64(5)	O2-Si1-O3	111.21(5)
O7-Si1-O3	104.93(5)	O7-Si1-O3	108.67(5)
O8-Si2-O6	112.05(6)	O8-Si2-O6	111.69(6)
O8-Si2-O2	107.02(7)	O8-Si2-O2	105.80(6)
O6-Si2-O2	112.00(6)	O6-Si2-O2	111.66(5)
O8-Si2-O3	107.65(7)	O8-Si2-O3	108.92(6)
O6-Si2-O3	106.73(6)	O6-Si2-O3	107.56(5)
O2-Si2-O3	111.36(6)	O2-Si2-O3	111.22(5)
O5-Si3-O7	111.59(5)	O5-Si3-O7	111.89(5)
O5-Si3-O1	106.55(5)	O5-Si3-O1	107.93(5)
O7-Si3-O1	108.55(5)	O7-Si3-O1	104.95(5)
O5-Si3-O4	113.42(5)	O5-Si3-O4	113.21(5)
O7-Si3-O4	105.67(5)	O7-Si3-O4	107.09(5)
O1-Si3-O4	111.03(5)	O1-Si3-O4	111.49(5)
O9-Si4-O1	108.66(7)	O9-Si4-O1	107.64(6)
O9-Si4-O6	111.94(6)	O9-Si4-O6	112.37(6)
O1-Si4-O6	107.53(6)	O1-Si4-O6	106.63(6)
O9-Si4-O4	105.93(6)	O9-Si4-O4	106.57(6)
O1-Si4-O4	111.10(5)	O1-Si4-O4	111.44(5)
O6-Si4-O4	111.68(6)	O6-Si4-O4	112.17(5)

+ Ca^{2+} at the Ca site lower than that obtained by the chemical analysis (i.e., 0.82 vs. 1.20 apfu). Nevertheless, Gualtieri et al. (1999a, 2000) found no evidence of Na^{+} + Ca^{2+} at the K site on the basis of Rietveld refinements of natural phillipsite.

The rearrangement of the extra-framework population at low temperature is likely due to the change in shape (and size) of the micropores by tetrahedral tilting, as shown by the anisotropy of the thermo-elastic unit-strain ellipsoid. Such an anisotropy is well reflected by the evolution of the "free diameters" (O ↔ O, Baerlocher et al. 2001) of the 8mR[010] (Fig. 6): O3 ↔ O3 is ~4.0 Å at 298 K and increases to ~5.3 Å at 100 K, in contrast O1 ↔ O1 is ~5.3 Å at 298 K and decreases down to ~3.9 Å at 100 K. This leads to an "inversion" of the ellipticity of the channel. It is especially interesting to note that the low-*T*-induced "compression" acts with a different mechanism than that displayed at high-pressure conditions. Gatta and Lee (2007) showed that phillipsite tends to accommodate the effect of hydrostatic pressure by cooperative rotation of the tetrahedra, increasing the ellipticity of the channel systems but maintaining the original elliptical configuration (i.e., without any "inversion" in ellipticity). As a consequence, the orientation of the unit-strain ellipsoid at high pressure (Gatta and Lee 2007) is different from that at low *T* (Fig. 6). The continuous and monotonic behavior of the unit-cell parameters between 298 and 100 K (Fig. 5) suggests that the reorganization of the extra-framework content in phillipsite changes continuously with temperature.

The distribution of the extra-framework population observed in this study at low *T* has not been observed in natural or in NH_4^{+}-, Na^{+}-, K^{+}-, Cs^{+}-, Mg^{2+}-, Ca^{2+}-, Ba^{2+}-, and Sr^{2+}-exchanged specimens of phillipsite (Steinfink 1962; Rinaldi et al. 1974; Stuckenschmidt et al. 1990; Garcìa et al. 1992; Gualtieri 2000; Gualtieri et al. 1999a, 1999b, 2000; Passaglia et al. 2000; Sani et al. 2002; Gatta and Lee 2007). This new structural model of the distribution of the extra-framework contents in phillipsite may help in understanding the "cation exchange capacity" (CEC) of this zeolite, as well as the discrepancies often found between the extra-framework population deduced on the basis of the CEC experiments and that calculated from chemical analyses. Further experiments on the local crystal chemistry of chemically different natural and cation-exchanged phillipsite by single-crystal X-ray diffraction are in progress.

ACKNOWLEDGMENTS

G.D.G. and N.R. thank the Italian Ministry of University and Research, MIUR-Project: 2006040119_004. The Associate Editor Darby Dyar, Wulf Depmeier, and an anonymous reviewer are thanked for the revision of the manuscript.

REFERENCES CITED

Alberti, A. (1978) Differenze di chimismo tra zeoliti idrotermali e sedimentarie. Rendiconti della Societa' Italiana di Mineralogia e Petrografia, 34, 471–484.

Armbruster, T. and Gunter, M.E. (2001) Crystal structures of natural zeolites. In D.L. Bish and D.W. Ming, Eds., Natural Zeolites: Occurrence, Properties, Application, 45, p. 1–57. Reviews in Mineralogy and Geochemistry, Mineralogical Society of America, Chantilly, Virginia.

Baerlocher, Ch., Meier, W.M., and Olson, D.H. (2001) Atlas of zeolite framework types, 5th edition, 302 p. Elsevier, Amsterdam.

Birch, W.D. (1989) Chemistry of Victorian zeolites. In W.D. Birch, Ed., Zeolites of Victoria, 2, p. 91–102. Mineralogical Society of Victoria Special Publication, Melbourne.

Černý, P. (1964) The phillipsite-wellsite-harmotome symmetry: Orthorhombic or monoclinic? Neues Jahrbuch für Mineralogie Monatshefte, 5, 129–134.

Černý, P., Rinaldi, R., and Surdam, R.C. (1977) Wellsite and its status in the phillipsite-harmotome group. Neues Jahrbuch für Mineralogie Abhandlungen, 128, 312–330.

Coombs, D.S, Alberti, A., Armbruster, T., Artioli, G., Colella, C., Grice, J.D., Galli, E., Liebau, F., Minato, H., Nikel, E.H., Passaglia, E., Peacor, D.R., Quartieri, S., Rinaldi, R., Ross, M., Sheppard, R.A., Tillmans, E., and Vezzalini, G. (1997) Recommended nomenclature for zeolite minerals: Report of the subcommittee on zeolite of the International Mineralogical Association Commission on New Minerals and Mineral Names. The Canadian Mineralogist, 35, 1571–1606.

de'Gennaro, M., Franco, E., Langella, A., Mirra, P., and Morra, V. (1982) Le zeoliti delle piroclastiti dei Monti Ernici. La phillipsite dei peperini. Acta Naturalia de l'Ateneo Parmense, 18, 163–176.

de'Gennaro, M., Langella, A., Cappelletti, P., and Colella, C. (1999) Hydrothermal conversion of trachytic glass to zeolite. Monocationic model glasses. Clays and Clay Minerals, 47, 348–357.

Des Cloizeaux, M. (1883) Note sur les caractères optique de la christianite et de la phillipsite. Bulletin de la Société Français de Minéralogie et de Cristallographie, 6, 305–311.

Farrugia, L.J. (1999) WinGX suite for small-molecule single-crystal crystallography. Journal of Applied Crystallography, 32, 837–838.
García, J., Gonzáles, M., Cáceres, J., and Notario, J. (1992) Structural modifications in phillipsite rich tuff induced by thermal treatment. Zeolites, 12, 664–669.
Galli, E. and Loschi-Ghittoni, A.G. (1972): The crystal chemistry of phillipsites. American Mineralogist, 57, 1125–1145.
Gatta, G.D. and Lee, Y. (2007) Anisotropic elastic behavior and structural evolution of zeolite phillipsite at high-pressure: A synchrotron powder diffraction study. Microporous and Mesoporous Materials, 105, 239–250.
Gottardi, G. and Galli, E. (1985) Natural Zeolites, p. 409. Springer-Verlag, Berlin.
Gualtieri, A.F. (2000) Study of NH_4^+ in the zeolite phillipsite by combined synchrotron powder diffraction and IR spectroscopy. Acta Crystallographica, B56, 584–593.
Gualtieri, A.F., Caputo, D., and Colella, C. (1999a) Ion-exchange selectivity of phillipsite for Cs^+: A structural investigation using the Rietveld method. Microporous and Mesoporous Materials, 32, 319–329.
Gualtieri, A.F., Passaglia, E., Galli, E., and Viani, A. (1999b) Rietveld structure refinement of Sr-exchanged phillipsites. Microporous and Mesoporous Materials, 31, 33–43.
Gualtieri, A.F., Passaglia, E., and Galli, E. (2000) Rietveld structure refinement of natural and Na-, K-, Ca-, and Ba-exchanged phillipsites. In C. Colella and F.A. Mumpton, Eds., Natural Zeolites for the Third Millennium, p. 93–110. De Frede, Naples, Italy.
Langella, A., Cappelletti, P., and de'Gennaro, R. (2001) Zeolites in closed hydrologic systems. In D.L. Bish and D.W. Ming, Eds., Natural Zeolites: Occurrence, Properties, Application, 45, p. 235–260. Reviews in Mineralogy and Geochemistry, Mineralogical Society of America and Geochemical Society, Chantilly, Virginia.
Langemann, L. (1886) Beitrage zur Kentniss der Mineralien: Harmotom, Phillipsit und Desmin. Neues Jahrbuch für Mineralogie, Geognosie, Geologie, und Petrefaktenkunde, 2, 83–141.
Ohashi, Y. (1982) STRAIN: A program to calculate the strain tensor from two sets of unit-cell parameters. In R.M. Hazen and L.W. Finger, Eds., Comparative Crystal Chemistry, p. 92–102. Wiley, New York.
Oxford Diffraction (2007) CrysAlis Software system, Xcalibur CCD system, Oxford Diffraction Ltd.
Passaglia, E. and Sheppard, R.A. (2001) The crystal chemistry of zeolites. In D.L. Bish and D.W. Ming, Eds., Natural Zeolites: Occurrence, Properties, Application, 45, p. 69–116. Reviews in Mineralogy and Geochemistry, Mineralogical Society of America and Geochemical Society, Chantilly, Virginia.
Passaglia, E., Galli, E., and Gualtieri, A.F. (2000) Variations of the physical and chemical properties in cation exchanged phillipsites. In C. Colella and F.A. Mumpton, Eds., Natural Zeolites for the Third Millennium, p. 259–267. De Frede, Naples, Italy.
Price, R.C., Gray, C.M., Nicholls, I.A., and Day, A. (1988) Cainozoic volcanic rocks. In J.G. Douglas and J.A. Ferguson, Eds., Geology of Victoria, p. 439–452. Geological Society of Australia (Victorian Division), Melbourne.
Rinaldi, R., Pluth, J.L., and Smith, J.V. (1974) Zeolites of the phillipsite family. Refinement of the crystal structures of phillipsite and harmotome. Acta Crystallographica, B30, 2426–2433.
Rinaldi, R., Smith, J.V., and Jung, G. (1975) Chemistry and paragenesis of faujasite, phillipsite, and offretite from Sasbach, Kaiserstuhl, Germany. Neues Jahrbuch für Mineralogie Monatshefte, 10, 433–443.
Sani, A., Cruciani, G., and Gualtieri, A.F. (2002) Dehydration dynamics of Ba-phillipsite: An in situ synchrotron powder diffraction study. Physics and Chemistry of Minerals, 29, 351–361.
Sheldrick, G.M. (1997) SHELX-97. Programs for crystal structure determination and refinement. University of Göttingen, Germany.
Sheppard, R.A. and Hay, R.L. (2001) Formation of zeolites in open hydrologic systems. In D.L. Bish and D.W. Ming, Eds., Natural Zeolites: Occurrence, Properties, Application, 45, p. 261–275. Reviews in Mineralogy and Geochemistry, Mineralogical Society of America and Geochemical Society, Chantilly, Virginia.
Steinfink, H. (1962) The crystal structure of the zeolite phillipsite. Acta Crystallographica, 15, 644–651.
Stuckenschmidt, E., Fuess, H., and Kvick, Å. (1990) Investigation of the structure of harmotome by X-ray (293 K, 100 K) and neutron diffraction. European Journal of Mineralogy, 2, 861–874.
Ulrich, G.H.F. (1870) Contributions to the mineralogy of Victoria. Mineral statistics of Victoria for the year 1869. Votes and Proceedings of the Legislative Assembly of Victoria, 1870/8 Appendix E, 52–67.
Vince, D. (1989) Melbourne Zeolite Region. In W.D. Birch, Ed., Zeolites of Victoria, 2, p. 1–30. Mineralogical Society of Victoria Special Publication, Melbourne.
Wilson, A.J.C. and Prince, E. (1999) International Tables for Crystallography Volume C. Kluwer Academic Publishers, Dordrecht.

Manuscript received June 4, 2008
Manuscript accepted July 23, 2008
Manuscript handled by Darby Dyar